Fabrication and Testing of Large Flats

Julius Yellowhair[*a], Peng Su[b], Matt Novak[b], Jim Burge[b]

[a]Currently at Sandia National Laboratories, 1515 Eubank SE, Albuquerque, NM 87123
[b]College of Optical Sciences, University of Arizona, 1630 E. University Blvd., Tucson, AZ 85721

ABSTRACT

Flat mirrors of around 1 meter are efficiently manufactured with large plano polishers and measured with Fizeau interferometry. We have developed technologies and hardware that allow fabrication and testing of flat mirrors that are much larger. The grinding and polishing of the large surfaces uses conventional laps driven under computer control for accurate and systematic control of the surface figure. The measurements are provided by a combination of a scanning pentaprism test, capable of measuring power and low order irregularity over diameters up to 8 meters, and subaperture Fizeau interferometry. We have developed a vibration insensitive Fizeau interferometer with 1 meter aperture and software to optimally combine the data from the subaperture tests. These methods were proven on a 1.6 m flat mirror that was finished to 6 nm rms irregularity and 11 nm rms power.

Keywords: large flat fabrication, metrology, optical manufacturing.

1. INTRODUCTION

For space-based or astronomical applications, large high performance flat mirrors are needed. However, large flat mirror fabrication poses significant challenges. The requirement on the radius of the mirror is at the same level as the requirement on surface irregularity (i.e. a few tens of nanometers). Classical fabrication and testing methods are well established for moderately sized optics (≤ 1 m). But the lack of scalability of classical methods makes the manufacture of flat mirrors much larger than 1 m less feasible. The standard method of characterizing flat surfaces uses Fizeau interferometers [1] that require comparison to a reference surface of similar size, but the development of such interferometers with meter type or larger apertures would be very expensive to produce. In addition, because large mirrors take months or even years to make, manufacturing becomes very costly.

The current state of the art for flat mirror fabrication uses continuous polishing [2-3]. Two advantages gained by using continuous polishing machines are the ability to produce multiple flat mirrors simultaneously and smoothly polishing out to the mirror edges. One disadvantage, however, is that mirrors can be no larger than about a third of the diameter of the lap. The largest continuous polishing machines are around 4 m in diameter. These machines can make up to 1.3 m diameter flat mirrors. For larger mirrors, facilities have to resort back to traditional polishing techniques.

The other limiting factor is that test data guide the polishing runs. The accuracy of the test limits the production of high quality mirrors. Large flat mirrors are typically tested interferometrically using the Ritchey-Common [4] and skip flat tests. Each test has advantages and disadvantages. Their disadvantages affect test efficiency and accuracy that is required in high quality large flat mirror manufacturing. In this paper, we address these limitations by developing accurate metrology and polishing techniques to produce large high precision flat mirrors.

We provide a brief introduction on the current fabrication technologies for manufacturing large high quality mirrors in Section 2. The testing technologies are reviewed in Section 3 and then described

* jeyello@sandia.gov

Optical Manufacturing and Testing VII, edited by James H. Burge, Oliver W. Faehnle, Ray Williamson,
Proc. of SPIE Vol. 6671, 667107, (2007) · 0277-786X/07/$18 · doi: 10.1117/12.736775

in more detail elsewhere [5-6]. Section 4 describes the manufacture and testing of a 1.6 m flat mirror and provides results on the finished mirror. Section 5 covers the feasibility of extending the fabrication and testing technologies that we developed to 4 m flat mirrors. The concluding remarks are provided in section 6.

2. FABRICATION TECHNOLOGIES

Mirror fabrication techniques include a vast array of polishing methods from the tried and true conventional or classical polishing methods to the modern computer controlled polishing used to make optical surfaces of varying sizes and shapes. The fabrication of large mirrors, in particular, is a time consuming process. The optician uses multiple machines, polishing tools, material and compounds, and specialized skill. In this section we provide a brief introduction to conventional and computer controlled polishing currently used in industry.

2.1. Conventional polishing

Conventional polishing techniques make use of proven and established polishing methods, which have been used for many decades [2-3]. Many polishing machines, tools, and techniques have been developed and refined over the years to increase efficiency and accuracy in shaping glass surfaces. Polishing pads, formed wax, or formed pitch, which make contact with the glass, are typically applied to the tool work surface. Various compounds are used during polishing as abrasives and wet slurry to help remove and smooth the glass surface. Conventional polishing techniques rely on controlling the shape of the polishing lap to adjust the entire surface of an optical element. These techniques can be used to make flat surfaces as well as a variety of other elements.

2.2. Computer controlled polishing

In the past few decades, computer controlled polishing has come to the forefront in optical manufacturing as the cost of computer control has come down and the flexibility of the method is realized [2-3]. Glass mechanics and polishing parameters are also now better understood; thus, repeatability and modeling of removal functions can be established. Polishing strokes can be optimized by performing well controlled polishing runs. Modeling and optimizing the polishing strokes then allow for accurate prediction of the outcome of a polishing run based on the polishing parameters selected. Important information related to the polishing tool dwell time and polishing hit can be then obtained.

3. TESTING TECHNOLOGIES

There are many metrology techniques in use for optical surface characterization. We developed two efficient tests that allowed us to accurately measure and monitor the flat surface during polishing and figuring. These test systems were used to guide the fabrication and provide measurements on the finished 1.6 m flat mirror. The two tests are briefly discussed below. Full descriptions of the test systems are given elsewhere [5-6].

3.1. Scanning Pentaprism Testing

The scanning pentaprism system, which used two pentaprisms co-aligned to a high resolution electronic autocollimator, provided an accurate optical slope test that measured power and other low order aberrations [7]. The scanning pentaprism was used during the late polishing and figuring stages of the 1.6 m flat to monitor the surface and guide the fabrication. It was also used as an absolute test for power on the finished mirror. This testing technique provided an accuracy of about 9 nm rms for power.

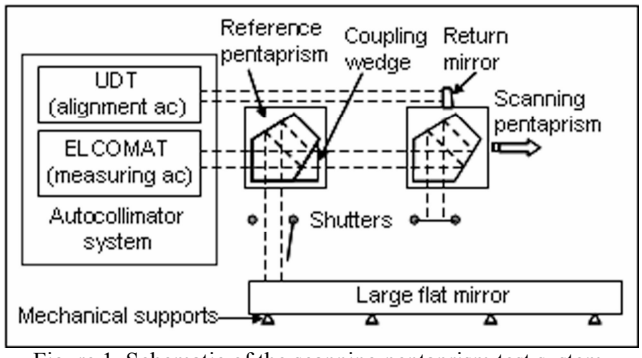

Figure 1. Schematic of the scanning pentaprism test system.

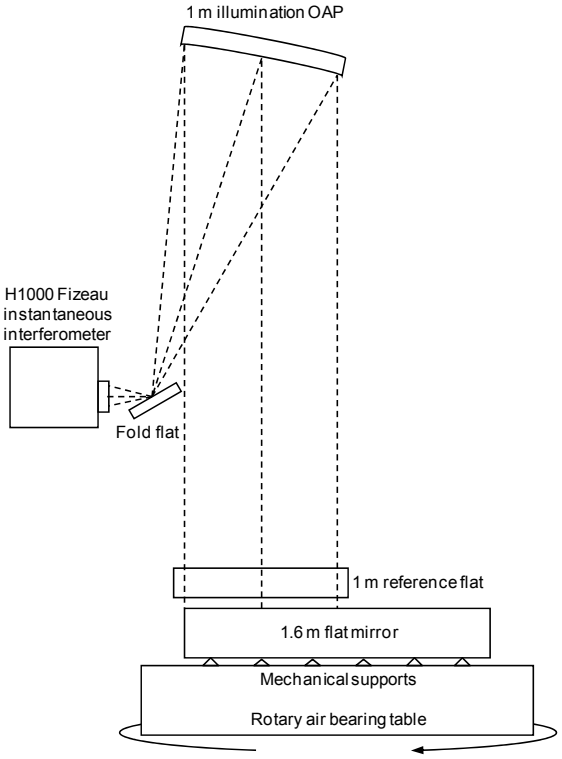

Figure 2. Schematic of the 1 m Fizeau interferometer with an OAP for beam collimation and an external 1 m reference.

3.2. Vibration Insensitive Fizeau Testing

We developed a large custom vibration insensitive Fizeau interferometer with a 1 m external reference to measure the higher order variations in the mirror surface and also guide the fabrication [6]. This test system used a 1 m beam combined with multiple overlapped subaperture measurements to provide complete coverage of the 1.6 m flat. Stitching and maximum likelihood estimation techniques were used to combine the subaperture measurements and obtain a full surface map. This measurement method provided an accuracy of 3 nm rms for surface irregularity.

We combined the scanning pentaprism data with the Fizeau data to provide state of the art surface measurement accuracy for large high performance flats. Both the scanning pentaprism system and the 1 m Fizeau reference were designed for kinematic positioning over the flat mirror during fabrication. The kinematic design allowed the flat mirror to remain fixed on the polishing table while the test systems were interchanged for complete surface testing *in-situ*.

4. MANUFACTURE OF A 1.6 M FLAT MIRROR

4.1. Introduction

The manufacture of large (> 1 m) high performance flat mirrors presents challenges because of the lack of enabling fabrication and testing technologies that economically provide measurement efficiency and accuracy. In this section, we describe the development of novel fabrication techniques that lead to manufacture a high performance 1.6 m flat mirror.

An important consideration for large mirrors is the design of proper mechanical supports, which must hold the large mirror to some small allowable deflection during polishing and testing. We discuss

the design of the mechanical supports for the 1.6 m flat mirror and provide an overview of the manufacturing sequence. Finally, we provide the measurement results on the finished mirror.

4.2. Mirror geometry

The mirror blank material was solid Zerodur® (Schott, Inc.) with 1.6 m diameter and 20 cm thickness. Figure 3 shows the mirror geometry, and Table 1 lists the geometry and material parameters for the mirror blank. The mechanical support design was optimized based these parameters. The mirror was supported from the back surface (zenith pointing) during the entire manufacturing process.

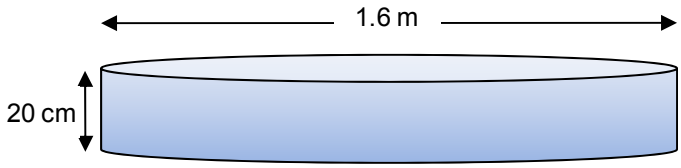

Figure 3. The 1.6 m Zerodur® flat mirror blank geometry.

Table 1. Parameters for the 1.6 m Zerodur® flat mirror blank.

Parameter	Value
Diameter, d	1.6 m
Thickness, t	0.20 m
Poisson's ratio, υ	0.243
Modulus, E @ 20°C	9.1×10^{10} N/m^2
Density, ρ	2530 kg/m^3
Total mass, m	1034 kg

4.3. Mirror support design

The polishing supports must control the mirror self weight deflection to some small allowable amount. Nelson et al. point out that for large (thin) mirrors, the number of support points and their arrangement control the mirror deflection with varying accuracy [8-9]. For the 1.6 m flat, Nelson's design for a 36 support point system arranged in a circular pattern was used as a baseline. This design was modeled and optimized using finite element analysis (FEA) software. The analysis showed that this support system maintained the mirror surface deflection to less than 3 nm rms.

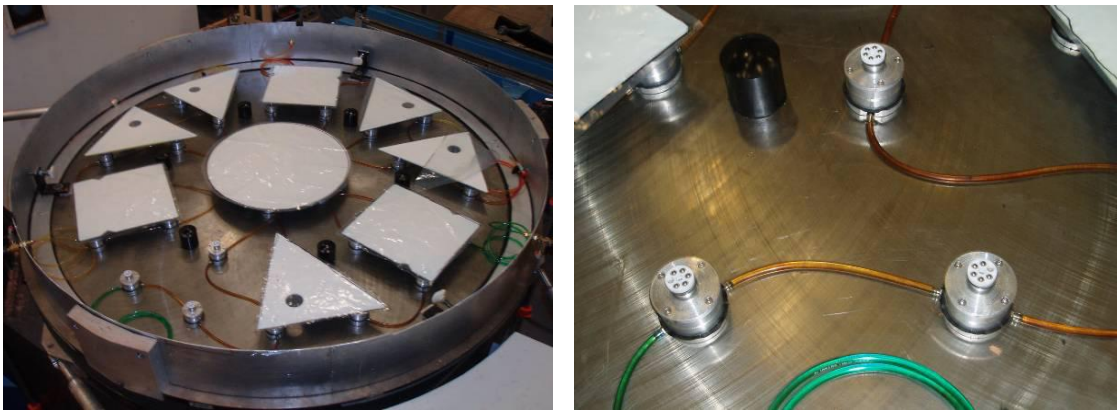

Figure 4. The mechanical support system used 36 hydraulic actuators to support the 1.6 m flat mirror (left), and a blow up of the plumbing of the hydraulic support points (right). The black cylinder (right figure) is one of six hard contact points; they do not contact the mirror in operation.

Our final polishing support design consisted of 36 hydraulic piston actuators laid out on a high performance air bearing polishing table as shown in Figure 4. Aluminum plates (square and triangular) were placed between the mirror and the actuators to protect the mirror back surface. Once the mirror was positioned on the hydraulic supports, it remained there the entire fabrication; polishing and testing were performed without removing the mirror. This approach lent itself to efficient manufacturing. In addition, this approach minimized transfers of the mirrors and, thus, risk of damaging the mirror.

4.4. Overview of the manufacturing sequence

The manufacture of large mirrors requires four phases: surface generation, grinding, polishing, and figuring [2-3]. We performed the grinding and polishing with a l00 cm tool. To perform the surface figuring, we developed a radial stroker, which drove smaller tools (size ranging from 15 to 40 cm diameters). We used polishing simulation software (described in Section 4.6.1) to help with the polishing decisions for given geometry, tool pressure, and other parameters. The software provided optimized tool stroke and dwell to reduce the surface zones. We used the scanning pentaprism system and the 1 m Fizeau interferometer to monitor the mirror surface and guide the fabrication.

4.5. Large tool polishing

The grinding and polishing were performed with a non-compliant, 100 cm diameter tool on a Draper machine. The tool applied about 0.3 pounds per square inch (psi) of pressure on the mirror. Grinding was performed with tiles set in pitch on the work surface side of the tool. For polishing, molded soft pitch in 10 cm squares was applied to the bottom of the tool with about 1 cm channels between the squares. Before each polishing run, the tool (with pitch) was first pressed out overnight on a flat surface. This step ensured a 'flat' tool at the beginning of a polishing run. To start polishing, polishing slurry was liberally applied to the mirror surface, and the large tool was placed on top. The motions of the tool were adjusted based on the measured surface data and historical behavior of the large tool with pitch. The tool was allowed to charge for a short time, after which it was timed for the actual polishing run. Charging the surface refers to the process of the polishing compound particles embedding themselves in pitch where they can remain active for a period of time and is essential for efficient polishing. Photographs of the 100 cm polishing tool and the polishing process are shown in Figure 5.

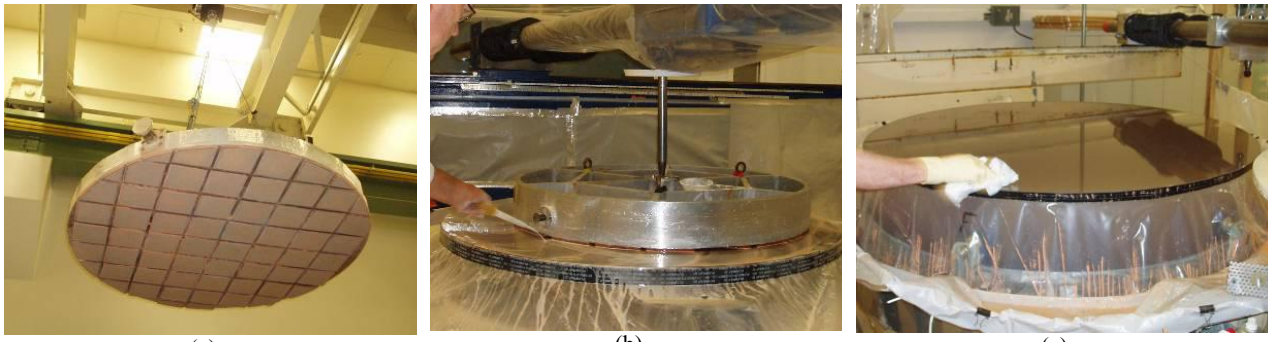

(a) (b) (c)

Figure 5. (a) Large (100 cm) tool with square tiles in pitch used for grinding. (b) Grinding/polishing with the large tool. (c) 1.6 m flat mirror polished to a smooth finish with a large tool.

4.6. Surface finishing with small tools

Large non-compliant polishing tools (> 75 cm diameter) can remove more glass than small tools. Therefore, a large tool can easily make global surface changes without introducing much surface ripple. However, large tools are not very useful in controlling the mirror surface shape, especially if the surface

is flat. Therefore, smaller tools with easily controlled and measured influence are used for surface figuring and finishing.

We used small tools with sizes ranging from 15 to 40 cm diameters at pressures 0.2 to 0.3 psi for surface figuring after failing with a 60 cm tool on the Draper machine. Channeled square molded pitch was applied to bottom side of each small tool. Before a tool was used, it was pressed out on a flat surface.

We developed a radial stroker, shown schematically in Figure 6, to drive the smaller tools. The radial stroker used two motors; one motor provided a variable tool stroke motion, and the other provided variable tool rotation of up to 8 revolutions per minute (rpm). The radial stroker was attached to the rail of the Draper polishing machine, which used a high quality rotary air bearing table to hold the mirror blank. Unlike large tools, the radial stroker with small tools allowed for zonal changes to the mirror surface. Depending on the zone width and height determined from the surface measurements, we chose the proper tool size to reduce the zone height by 40 to 50% in a single run. This conservative approach avoided removing too much glass and creating a low zone. A low zone correction requires the entire surface to be brought down to that level. The small tool was positioned over the high zones by moving the Draper machine rail, which normally would provide stroke for large polishing tools. Polishing simulation software, used to optimize the polishing tool stroke and dwell, enabled computer control to correct the surface figure.

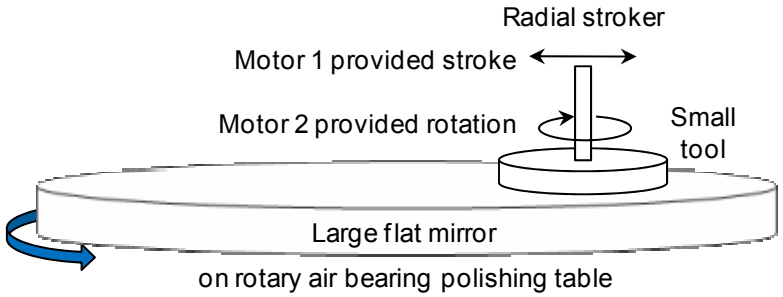

Figure 6. Schematic of the radial stroker and figuring with small tools. The radial stroker was attached to the Draper machine rail. Two motors provide variable tool stroke and rotation.

4.6.1. Computer controlled polishing

We developed computer controlled polishing for surface figuring through polishing simulation software. The computer control came from the choice of polishing strokes based on computer simulation and optimization. The polishing simulation software is based on the finite element modeling of the lap and glass mechanics and assumed Preston's relation, that glass removal rate is proportional to pressure and velocity between the tool and the mirror. The software differed from most by allowing the use of a rotating tool with a removal function that varies significantly with position of the tool on the mirror [10]. The computation of the removal function at any point on the mirror is made by numerically integrating Preston's relation over the tool stroke position and mirror rotation angle. We used the software to simulate polishing for a given set of input parameters (i.e. tool size, pressure and geometry, tool and mirror rotation speeds, etc.). Parameters such as the tool dwell, stroke and position were then optimized for a particular surface zone. Each surface zone required its own data file, which were combined to simulate the net effect on the mirror. The design of the full polishing run was then given to the optician to execute on the mirror.

To predict the surface removal, we first calibrated the Preston's constant. Preston's equation is related to the rate of the material removal caused by the tool velocity and pressure for each point on the mirror relative to the glass:

$$R(p,v) = K \times p \times v \tag{1}$$

where R is the local removal rate, K is Preston's proportionality constant (units μm/hr/psi/m/s), p is the local tool pressure, v is the instantaneous linear velocity of the tool relative to the mirror surface.

To use the software successfully, the Preston's constant first required calibration by measuring the effects of the polishing strokes and tool dwell. A simple polishing run was designed and simulated with the software. The simulation was then executed on the mirror. The mirror surface was measured before and after this polishing run. Preston's constant was adjusted in software until the simulated surface removal matched the actual removal amplitude. The resulting constant was then recorded and stored for future simulations. A typical value for our process was 15 μm/hr/psi/m/s.

Figure 7a shows an example of designing removal functions for a measured surface radial profile exhibiting two zonal errors. The ideal removal profile is an inverted surface radial profile reduced in height. Figure 7b shows the surface after applying the removal functions, which results in a new surface with smaller zone heights.

Once the profiles of the ideal removal functions were established, the goal was to duplicate the profiles by choosing the right tool size, pressure, and rotation rates and then optimizing tool stroke and dwell.

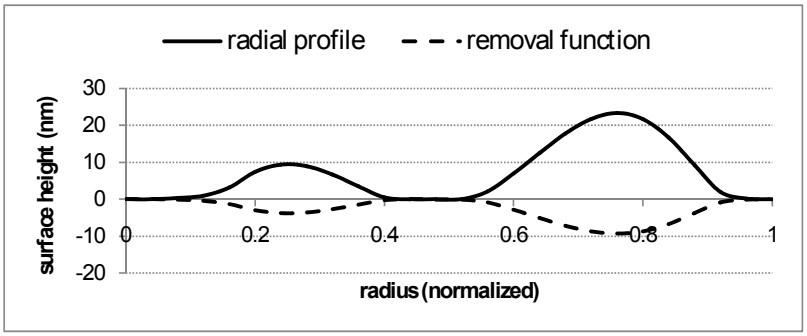

(a)

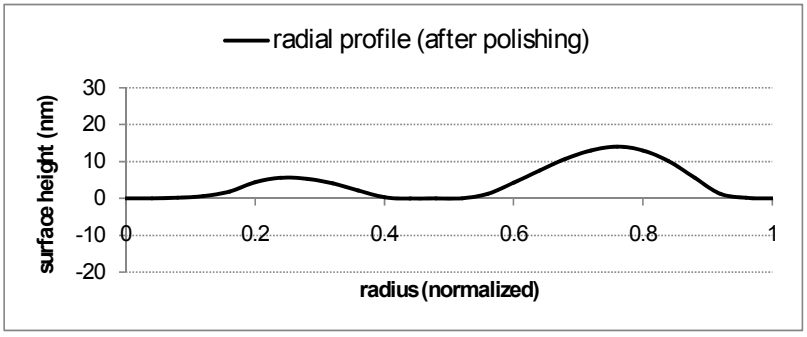

(b)

Figure 7. Example of reducing zone heights with proper design of removal functions assuming only zonal errors are present in the surface. (a) Initial measured surface radial profile showing two zones and the removal functions designed for each zone. (b) Surface after applying the removal functions.

Figure 8 shows a real example of the result of a polishing simulation, which consisted of multiple removal functions with varying tool sizes and dwells, and the actual surface removal after the computer controlled polishing was applied to the mirror. The actual removal departs from the predicted for two reasons: smoothing and non-linear behavior [10]. The polishing tool provides natural smoothing of the mirror surface. In addition, Preston's constant may vary with velocity and pressure, $K(p,v)$, resulting in non-linear removal effects. Although the software has evolved to include nonlinear effects, this option was not used, because the magnitude of the nonlinear effects was not known.

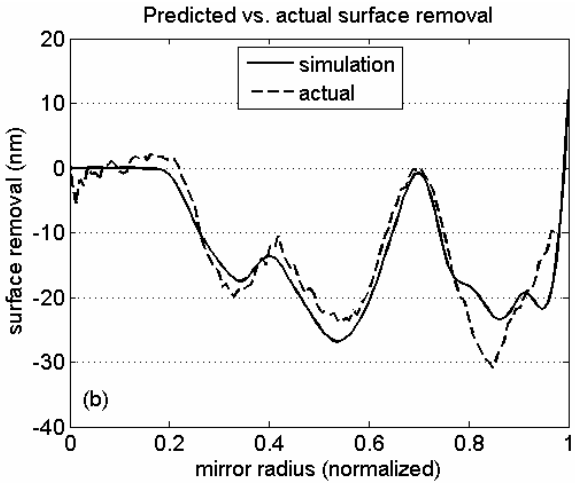

Figure 8. Comparison of a simulated and actual surface removal on the 1.6 m flat while it was in production.

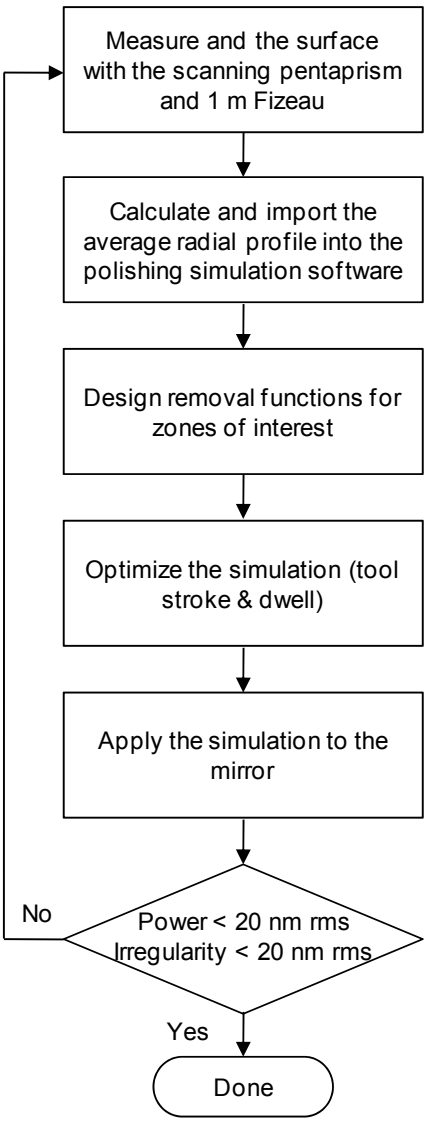

Figure 9. Flowchart diagram of the closed loop computer controlled polishing method.

Computer controlled polishing procedure

The method of computer controlled polishing was operated in a closed loop. A summary of the steps for completing a computer controlled run is given next.

First, the mirror surface was measured with the scanning pentaprism system and the 1 m Fizeau interferometer, and the average radial profile of the mirror was calculated. The average radial profile was imported into the polishing simulation software along with the expected polishing parameters. In software the surface removal function for each zone was generated and optimized. The target reduction for each zone was typically 40 to 50% of the maximum zone height. The surface removal on the measured average radial profile was then simulated, and the result was evaluated. Finally, the optimized polishing design was applied to the mirror. After the polishing run was complete, the process was repeated.

Figure 9 shows this same sequence in a flowchart. Typically, polishing runs lasted three to five hours. This included time to change out polishing tools and move the tool to other zones on the mirror. Multiple iterations of the above sequence were carried out. In the next section, we present measurements obtained after the final run. The method of closed loop computer controlled polishing convergence of the surface figure was relatively rapid (an average of about 50 nm rms per week for power as shown in Figure 13).

4.6.2. Scanning pentaprism measurements

The scanning pentaprism test result on the finished mirror is shown in Figure 10. The measurement was made along a single diagonal line on the mirror. Forward and backward scans were performed and the data were averaged. Only slope functions derived from rotationally symmetric Zernike polynomials were fitted to the data. The linear component of the fit then gives power. This measurement resulted in 11 nm rms power with measurement uncertainty of 9 nm rms. The large slopes due to surface irregularity were not represented well with low order polynomials. Irregularity was more accurately measured interferometrically with the 1 m Fizeau interferometer.

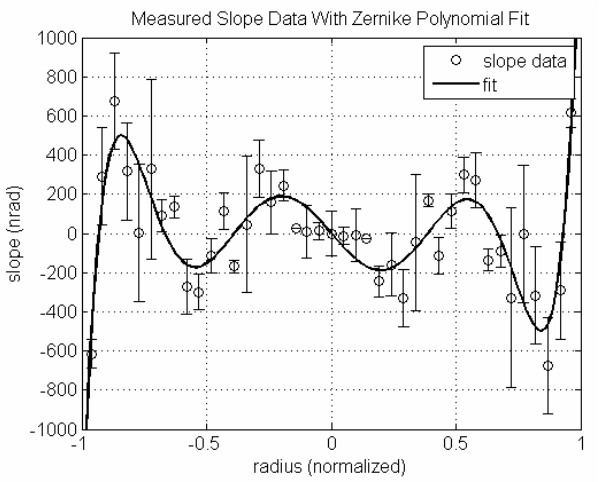

Figure 10. Measured slope data on the finished mirror with the scanning pentaprism along a single line and low order polynomial fit to the slope data. The linear component of the polynomial fit gives power in the surface (11 nm rms).

4.6.3. Fizeau measurements for surface irregularity

The surface map, shown in Figure 11, is the result of the 1 m Fizeau interferometer test on the finished mirror. A total of 24 overlapping subaperture measurements were acquired through multiple rotations of the reference and test surfaces. The subaperture measurements were then combined using the maximum likelihood estimation to get a full surface map [11]. Up to 188 mostly rotationally symmetric Zernike terms were used to reconstruct the surface. Removing power and astigmatism left a surface irregularity of 6 nm rms with measurement uncertainty of 3 nm rms. The results from stitching are not provided here but can be found elsewhere [12].

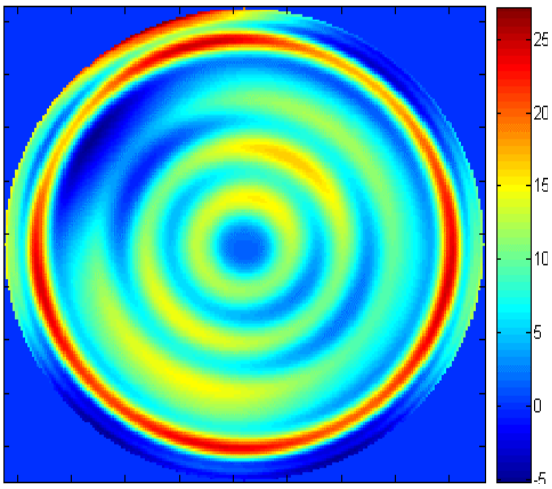

Figure 11. Result of the 1 m Fizeau measurement on the finished mirror. 24 subaperture measurements were acquired and combined using maximum likelihood estimation (6 nm rms surface irregularity). The units are nanometers.

4.7. Demonstration of the flat mirror with 11 nm rms power and 6 nm rms surface irregularity

Figure 12 demonstrates the final surface map, which is the combination of the results from the scanning pentaprism and Fizeau tests on the finished mirror: 11 nm rms power and 6 nm rms surface irregularity. The final surface was characterized to 12.5 nm rms and 57 nm peak to valley.

By continuing with the closed loop computer controlled polishing described in section 4.6.1 and based on the sensitivities of the test systems, we estimated 9 nm rms power and 3 nm rms surface irregularity to be achievable for 2 m class flat mirrors. Due to time constraints these numbers were achieved for the 1.6 m flat.

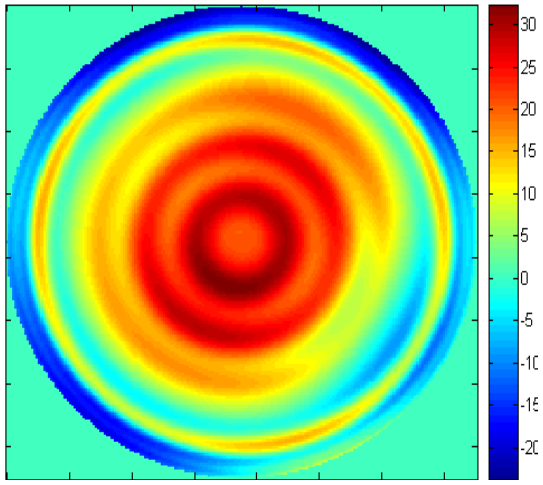

Figure 12. The final surface map showing combined power with surface irregularity from the scanning pentaprism and 1 m Fizeau tests on the finished mirror. The units are nanometers.

Figure 13 demonstrates the rapid convergence of surface power on the 1.6 m flat mirror after implementing our computer controlled polishing. Measurements on the left side of the vertical dashed line were taken during classical large tool polishing before our computer controlled polishing. The classical polishing method used a 60 cm polishing tool to make corrections to the mirror surface. This method managed to bring the surface to about 60 nm rms power before reversing direction on the error. After several more polishing runs with the 60 cm tool and a dramatic increase in the surface power, we switched to the closed loop computer controlled method.

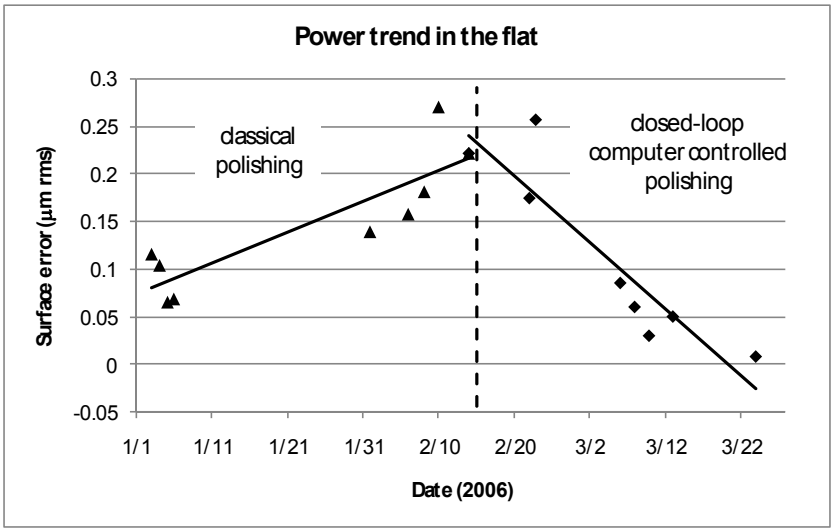

Figure 13. Power trend in the 1.6 meter flat (over about three months) as measured with the scanning pentaprism system. The power trend shows rapid convergence after implementing the polishing software aided computer controlled polishing.

5. MANUFACTURING PLAN FOR A 4 M FLAT MIRROR

A key advantage of our manufacturing methodology described is that it is scalable to larger mirrors. In this section we discuss the feasibility of extending our methodology to 4 m class mirrors.

5.1. Mirror geometry

Zerodur® (Schott Glass, Inc.), ULE® (Corning, Inc.), and fused quartz are common low expansion glass materials for large mirror blanks. Each glass type has properties that make it ideal for specific applications. Zerodur®, for example, has excellent opto-thermal properties and chemical resistance, so it is typically chosen for space programs and other extreme applications. For the purpose of the analysis below, we assumed a solid Zerodur® mirror blank with a thickness of 10 cm shown in Figure 14 (40:1 aspect ratio).

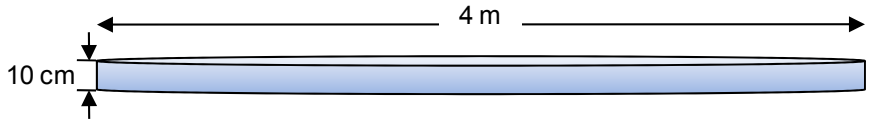

Figure 14. Solid Zerodur® 4 m flat mirror geometry.

5.2. Mirror support

Using the same approach described by Nelson et al. as a baseline (see Section 4.3), a support system with 120 points, arranged on five rings, was modeled and optimized for a mirror geometry described above. The support system arrangement is shown in Figure 15. The FEA modeling showed this support arrangement will maintain the mirror surface deflection to about 12 nm rms.

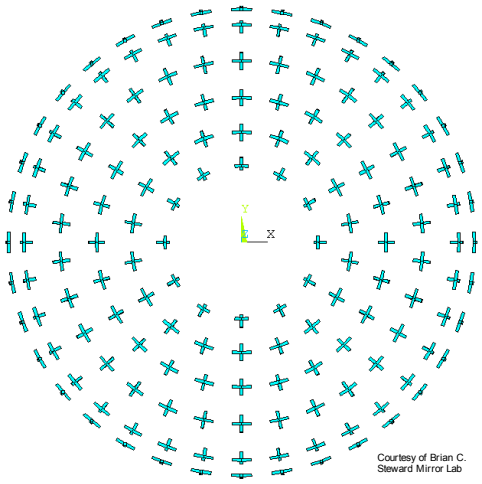

Figure 15. A five ring support design for a 4 m mirror. This design will maintain the mirror deflection to about 12 nm rms.

5.3. Overview of the manufacturing sequence

Many of the same processes that were established during the manufacture of the 1.6 m flat mirror can be used in larger mirror fabrication. After the mirror surface generation, the manufacturing process might proceed as follows (and shown in Figure 16):

- Use a large non-compliant tool (≥ 100 cm) with tiles to grind and then with pitch to polish the surface to a smooth finish, minimize power and asymmetrical surface variations.
- Use efficient metrology to make surface measurements, monitor global surface changes, and guide the initial polishing.
- Switch to smaller tools (40 to 80 cm diameter) for figuring after the surface obtains a smooth finish and power is less than 100 nm rms.
- Use the scanning pentaprism and 1 m Fizeau tests to monitor the surface and guide the remaining fabrication.
- Use polishing simulation software make decisions on polishing and figuring.

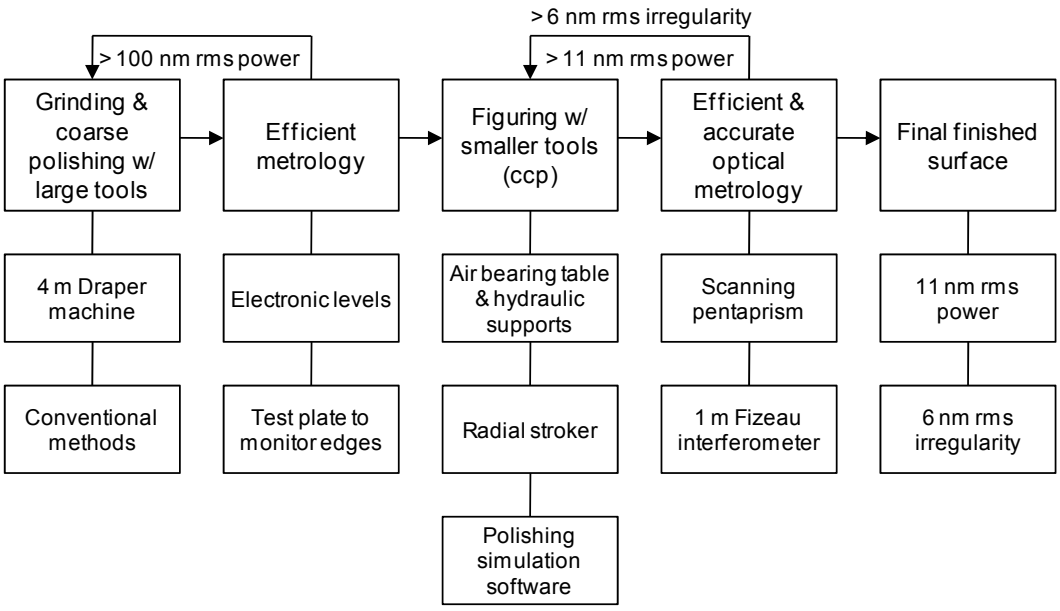

Figure 16. Potential manufacturing sequence for large high performance flat mirrors.

5.4. Limitations

5.4.1. Fabrication: polishing and figuring

Our facility is currently limited to handling 4 m mirrors. Additional modifications to our polishing table are necessary to accommodate mirrors larger than 4 m.

In addition, our large tool is limited to 100 cm in diameter. A 230 cm diameter or larger tool, after characterization, can be used on a 4 m mirror for initial polishing. In some cases, polishing techniques proven for smaller mirrors do not work for large mirrors. As the tool size increases, so does the pressure it exerts on the mirror surface. This alone may change the expected polishing outcome. To succeed with manufacturing large high quality flats, careful planning and design is essential with special attention to gaining experience with tools and their effect on mirrors during fabrication.

5.4.2. Surface slope testing

For a given magnitude surface error (e.g. 20 nm rms astigmatism) the surface slope errors are inversely proportional to the mirror size. Thus, slope errors for a large mirror must become smaller to maintain the same performance as a smaller one. For power, the edge slope error is inversely proportional to the diameter of the mirror by

$$\Delta\theta = \frac{8s}{D}, \tag{2}$$

where s is the peak to valley power or sag in the mirror surface, D is the diameter of the mirror.

If the slope test is expected to measure 60 rms power in a 2 m mirror, then the edge slopes are 1 μrad. For the same specification on power for a 4 m mirror, the edge slopes become 0.5 μrad. The sensitivities of the test systems must be improved to fabricate larger mirrors accurately.

5.4.3. Large Fizeau test

In the current Fizeau test the 1 m reference flat and test mirror are fixed in lateral translation. This configuration limits how large a mirror we can test by subsampling (≤ 2 m). To measure larger mirrors, another degree of freedom in lateral translation is needed for the reference flat. Figure 17a shows the current subaperture sampling arrangement to measure 2 m or smaller flat mirrors. The reference flat remains fixed and the test mirror is rotated underneath to get full coverage. For a 1.6 m flat mirror eight subaperture measurements are enough to get full coverage of the test mirror [6]. This type of sampling arrangement is insufficient for flat mirrors larger than 2 m. Figure 17b shows an example of subsampling a 4 m mirror after introducing lateral translation of the 1 m reference flat. In this example, the reference flat is translated to three positions and the test mirror is rotated underneath to acquire 25 subaperture measurements and provide full coverage of the mirror. All 25 measurements must be combined to get a full synthetic surface map.

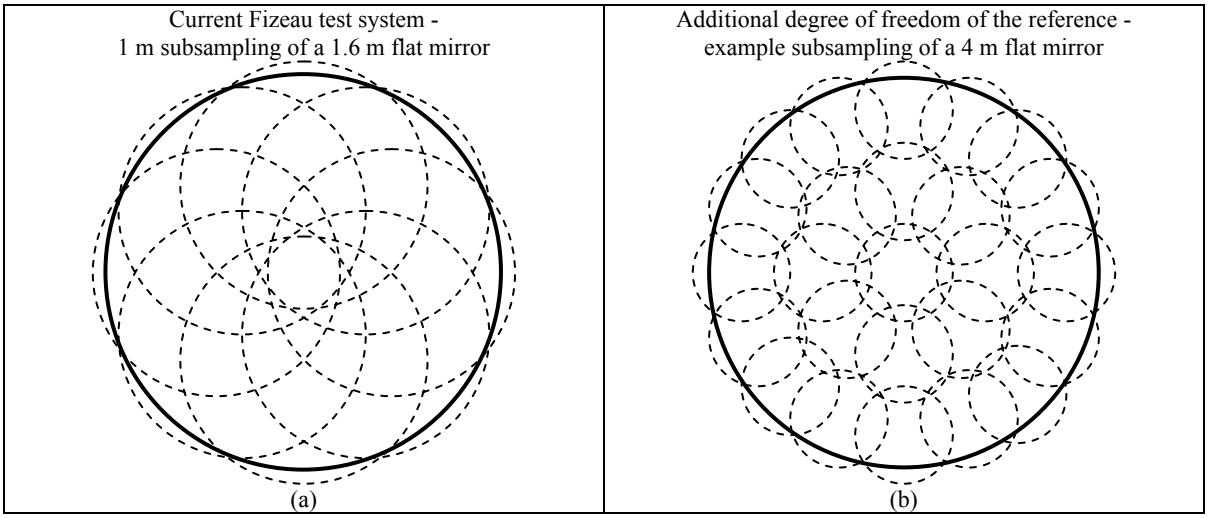

Figure 17. (a) 1 m subaperture (dashed circular outlines) sampling on the 1.6 m flat mirror, and (b) on a 4 m flat mirror. Multiple subaperture sampling provides full coverage of the large mirror. Combining the subaperture measurements produces a full synthetic map.

Errors in stitching the subaperture measurements increase as more subapertures are combined. The increase in subaperture measurements limits the accuracy of the test system. However, the quality of the test in terms of slope, power spectral density or structure function is not degraded

6. CONCLUSION

The manufacture of large flat mirrors is challenging. We found classical polishing alone does not enable the manufacture of large high performance flat mirrors much larger than 1 m diameter. We reported on the methodology and enabling technologies for fabricating and testing large high performance flat mirrors. We demonstrated the methodology on a 1.6 m flat mirror that measured 11 nm rms in power and 6 nm rms in surface irregularity on the finished mirror. Our developed fabrication and testing technologies are scalable for manufacture of flat mirrors as large as 8 m in diameter with proper tool design and selection. Our discussion of limitations showed the accurate manufacture of a 4 m flat mirror is within our current capability.

ACKNOWLEDGEMENTS

The authors gratefully acknowledge these individuals who have contributed tremendously to this work: Jose Sasian, Brian Cuerden, Robert Stone, Norman Schenck, Robert Crawford, Thomas Peck, Chunyu

Zhao, David Hill, Scott Benjamin, Marco Favela, Daniel Caywood, and numerous graduate and undergraduate students.

REFERENCES

1. M. V. Mantravadi, "Newton, Fizeau, and Haidinger interferometers," in *Optical Shop Testing*, D. Malacara, Ed. (Wiley, 1992), pp. 1-49.
2. D. Anderson, J. Burge, "Optical fabrication," in *Handbook of optical engineering*, D. Malacara , Ed., New York: Mercel Dekkar (2001), pp. 915-955.
3. H. H. Karow, Fabrication Methods for Precision Optics, New York: Wiley-Interscience (1993).
4. J. Ojeda-Castaneda, "Foucault, wire, and phase modulation tests" in *Optical shop testing*, D. Malacara, Ed. (Wiley, 1992), pp. 265-320.
5. J. Yellowhair, J. H. Burge, "Analysis of a scanning pentaprism system for measurements of large flat mirrors," accepted for publication in App. Opt. (2007).
6. J. Yellowhair, College of Optical Sciences, University of Arizona, 1630 East University Boulevard, Tucson, AZ 85721, R. Sprowl, P. Su, R. Stone, and J. H. Burge are preparing a manuscript to be called "Development of a 1-m vibration-insensitive Fizeau interferometer."
7. J. Yellowhair, J. H. Burge, "Measurement of optical flatness using electronic levels," accepted for publication in Opt. Eng. (2007).
8. J. E. Nelson, J. Lubliner, T. S. Mast, "Telescope mirror supports: plate deflections on point supports," SPIE **322**, 212 (1982).
9. P. R. Yoder, "Opto-Mechanical Systems Design," Dekker (1986).
10. J. H. Burge, "Simulation and optimization for a computer-controlled large-tool polisher," in *Optical Fabrication and Testing*, OSA Technical Digest **12**, 43 (1998).
11. P. Su, J. Burge, R. Sprowl, J. Sasian, "Maximum Likelihood Estimation as a General Method of Combining Sub-Aperture Data for Interferometric Testing," Proc. SPIE **6342,** 63421X (2006).
12. C. Zhao, R. Sprowl, M. Bray, J. H. Burge, "Figure Measurements of a Large Optical Flat With a Fizeau Interferometer and Stitching Technique," Proc. SPIE **6293,** 62930K (2006).